

# Effect of Distributor Plate Configuration on Pressure Drop in a Bubbling Fluidized Bed Reactor

## ABSTRACT

A pilot scale fluidized bed system was used to study the effect of distributor plate shape and conical angle on the pressure drop. Five distributor plates (flat, concave with 5°, concave with 10°, convex with 5° and convex with 10°) were used in the study. The system was tested at two levels of sand particle size (a fine sand of 198  $\mu\text{m}$  and coarse sand of 536  $\mu\text{m}$ ), various bed heights (0.5 D, 1.0 D, 1.5 D and 2.0 D cm) and various fluidization velocities (1.25, 1.50, 1.75 and 2.00  $U_{mf}$ ). The pressure drop was affected by the shape and the conical angle of distributor plate, sand particle size and bed height. Less than theoretical values of the pressure drop were observed with the 10° concave distributor plate at lower fluidizing gas velocities for all bed heights. A decrease in the angle of convex and an increase in the angle of concave resulted in a decreased pressure drop. Greater values of pressure drop were obtained with larger sand particles than those obtained with small sand particles at all fluidizing velocities and bed heights. For all distributor plates, increasing the bed height increased the pressure drop but decreased the ratio of pressure drop across the distributor to the pressure drop across the bed ( $\Delta P_D/\Delta P_B$ ). There was no variation in the pressure drop in the freeboard. Fluidizing gas velocities higher than 1.25  $U_{mf}$  should be used to for a better fluidization, improved mixing and avoiding slugging of the bed.

**Keywords:** Fluidized bed, pressure drop, fluidization velocity, particle size, bed height, distributor plate, concave, convex, angle, location.

## 1. INTRODUCTION

Cereal straws have come in recent years to be regarded as an unwanted companion of the cereal crops. Their use as animal feedstuff, livestock bedding materials, erosion control agents,

building materials, chemical sources, pulping material and craftwork materials have diminished(Pavia et al., 2004). These residues can be better utilized by converting them directly to energy(by combustion) or to energy carrying products (by gasification, pyrolysis and fermentation).These products could be used to meet farm energy needs or be transported for use of farm (FAO, 2013).The organic carbon formed within the biomass during photosynthesis is released during combustion of biomass (or biofuels driven from biomass), making biomass a carbon neutral energy source (Surisetty et al., 2012; Goyal et al., 2008). The conversion of biomass into usable energy sources represents a vital method of reducing fossil fuel dependence and greenhouse gas emission. The low levels of impurities in biomass lead to lower SO<sub>x</sub> and NO<sub>x</sub> emission during combustion and thus reduced contribution to acid rain (Wood and Layzell, 2003).

Gasification as a thermochemical conversion process can be used to convert cereal straws into syngas. One of the important features of gasification of cereal straws is that the reactiontemperature can be kept as low as 600°C, thereby preventing sintering and agglomeration of theash which occurs during the high temperature (100-1200°C) of the combustion process (Ergudenler and Ghaly, 1993).Fluidized bed reactors have been shown to be more suitablethan moving or fixed bed reactorsfor the gasification of low density fuels such as crop residues because they are less prone toslagging.

The application of fluidized bed gasification technology to cereal straw is increasing rapidly (Ergudenler and Ghaly, 1992; Khan et al., 2009). Effective gasification of straw requires rapid mixing of the fuel material with the inert sand of the bed in order to obtain a uniform distribution of the fuel particles, a better chemical conversion and a uniform temperature throughout the bed (Rowe and Nienow, 1976; Mansarey and Ghaly, 1999; Surisetty et al., 2012). However, mixing problems in fluidized bed systems become very severe when fuel particles vary both in size and density resulting in material segregation (Yoshida et al., 1980; Ergudenler and Ghaly, 1992; Nemtsov and Zabaniotou, 2008). One of the main causes of segregation is the out of balance forces during the periodic disturbances with the passage of the bubbles due to differences in density (Nemtsove and Zambaniotou, 2008).

The gas distributor plate is one of the most critical features in the design of a fluidized bed reactor (Ergudenler and Ghaly, 1992). The use of a suitable gas distributor is essential for satisfactory performance of gas-solid fluidized beds (Ghaly and MacDonald, 2012). Understanding of solids mixing and flow characteristics of gases and solids near the grid region of a fluidized bed reactor is vitally important from the standpoint of design and scale up of gas distribution systems (Bonnioi et al., 2009). The presence of stagnant zones near grid region can cause hot spots resulting in agglomeration and eventual reactor failure (Ergudenler and Ghaly, 1993). Ghaly and MacDonald (2012) developed a concave/convex type distributor plate which provided good mixing characteristics and a complete bed material turnover that prevented the occurrence of stagnant zones near the grid region.

The pressure drop across the bed is another important factor to consider when designing a fluidized bed gasification system. The quality of fluidization taking place in the bed can be deduced from the bed pressure drop. Theoretically, the pressure drop across the bed should be equal to the weight of the bed particles per unit cross-sectional area of the fluidizing column as follows (Sundaresan, 2003; Basu, 2006):

$$\Delta P = \frac{W}{A} \quad (1)$$

The weight of the bed particles (W) is calculated as follows:

$$W = H A (\rho_p - \rho_g)(1 - \epsilon_{mf}) \quad (2)$$

Equations 1 and 2 can be combined as follows:

$$\Delta P = H (\rho_p - \rho_g)(1 - \epsilon_{mf}) \quad (3)$$

Where:

- $\Delta P$  = Pressure drop (kPa)
- $W$  = Weight (kg)
- $A$  = Cross sectional area ( $m^2$ )
- $g$  = Gravitational constant ( $9.8 m/s^2$ )
- $H$  = Height of fixed bed (m)
- $\rho_p$  = Density of the particle ( $kg/m^3$ )
- $\rho_g$  = Density of fluidizing gas ( $kg/m^3$ )
- $\epsilon_{mf}$  = Bed voidage at minimum fluidization (-)

However several studies showed that the pressure drop across the fluidized bed is slightly larger than the weight of the bed particles per unit cross-sectional area. Menon and Durian (1997) reported that the pressure drop across the fluidized bed reactor is normalized by the weight of the entire bed per unit area. Taghipour et al. (2005) reported that the overall bed pressure drop decreased significantly at the beginning of fluidization and fluctuated around steady state due to bubbles being continuously split and coalesce in a transient. Kawaguchi et al. (1998) reported that there will be strong pressure fluctuations when bubbling and slugging occurs. The authors indicated that both experimental and calculated pressure drops were smaller than the value estimated from the gravity of the particles because the particles present do not fluidize uniformly.

Pressure drop fluctuations have been observed in gas fluidized beds is a good method determining fluidization quality. Large fluctuations may indicate slugging and no fluctuations at all may indicate severe channeling in the bed. Moderate fluctuations indicate good fluidization. Therefore, for a good gas particles distribution, distribution plates are designed such that gas passing through them experience sufficient pressure drop to prevent the formation of channels in the bed. Geldart and Beayens (1985) have shown that the pressure drop ( $\Delta P$ ) across a distributor plate can be calculated as follows:

$$\Delta P_d = \frac{\rho_g U^2}{2 C_d^2 F^2} \quad (4)$$

Where:

$\Delta P_d$  = Pressure drop across distributor plate (kPa)

$\rho_g$  = Density of fluidizing gas ( $\text{kg/m}^3$ )

$U$  = Fluidizing gas velocity (m/s)

$C_d$  = Discharge coefficient (-)

$F$  = Fractional free area (-)

The discharge coefficient ( $C_d$ ) depends on the shape of the plate orifice (hole) fractional free area (F). Also, the thickness of the plate affects the discharge coefficient and hence the pressure drop. The thicker the distributor plate, the lower the pressure drop across the plate (Qureshi and Creasy, 1979). Clift (1986) showed that for square-edged circular orifice with diameter ( $d_0$ ) much larger than the plate thickness ( $t_p$ ),  $C_d$  can be taken as 0.6 for  $t_p/d_0$  greater than 0.09. Qureshi and Creasy (1979) gave the following correlation between  $C_d$  and  $t_p/d_0$ :

$$C_d = 0.82 \left[ \frac{t_p}{d_o} \right]^{0.13} \quad (5)$$

Where:

$d_o$ = Orifice diameter (cm)

$t_p$ = Plate thickness (cm)

The pressure drop across the distributor plate can be calculated as a function of the bed pressure drop and aspect ratio using the following correlation (Qureshi and Creasy, 1979):

$$\frac{\Delta P_D}{\Delta P_B} = 0.01 + 0.2 \left[ 1 - \exp \left( -0.5 \frac{D}{H_{mf}} \right) \right] \quad (6)$$

Where:

$D$  = Bed diameter (cm)

$H_{mf}$ = Bed height at minimum fluidization (cm)

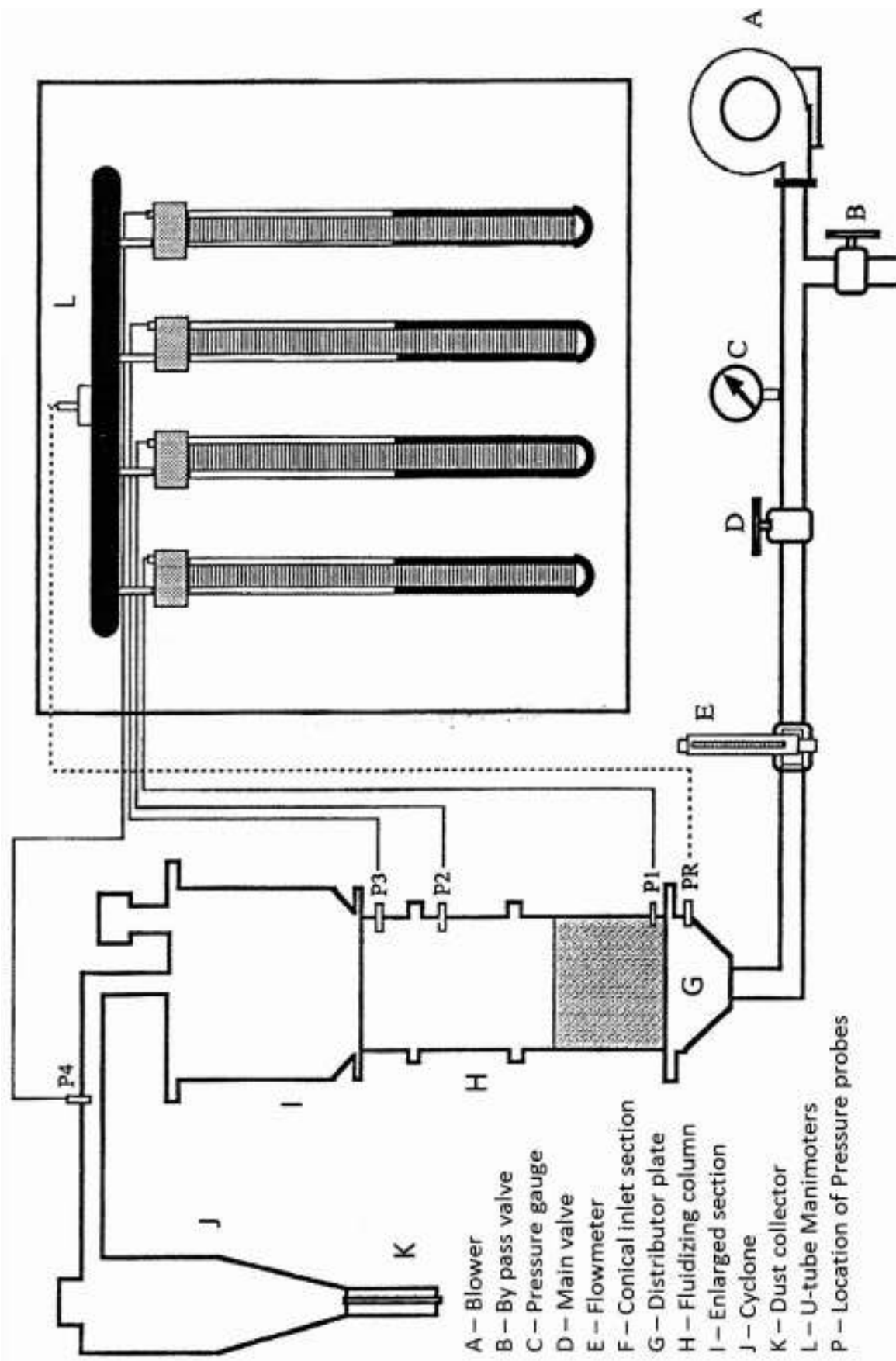
$\Delta P_d$ = Pressure drop across distributor plate (kPa)

$\Delta P_b$ = Bed pressure (kPa)

Pressure drop across the distributor plate can be used to deduce information regarding solids circulation patterns and to show whether the performance of the plate is changing with time or not. The main aim of the study was to investigate the effects of distributor plates configuration (shape and angle) on pressure drop in a bubbling fluidized bed gasification system operating at room temperature and various levels of sand particle size, bed height and fluidization velocity.

## 2. EXPERIMENTAL APPARATUS

The experimental apparatus used in this study is shown in Figure 1. The system consisted of: (a) a fluidized bed reactor, (b) an air supply unit, (c) a cyclone and (d) a pressure drop measurement system. With reference to Figure 1, the following are detailed descriptions of the system components.



133

134 Figure 1. Experimental Apparatus

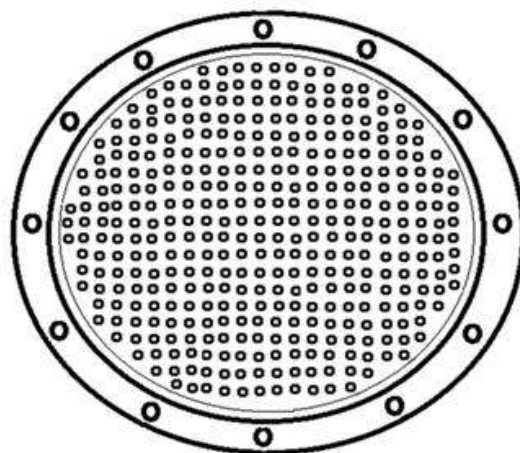
## 2.1. Fluidized Bed Reactor

The fluidized bed reactor consisted of: (a) a support stand, (b) a conical inlet section, (c) a distributor plate, (d) a fluidizing column, (e) a disengagement section and (f) an outlet duct.

The support stand was constructed of 38 mm steel angle iron. A horizontal square structure made of four 380 mm long angle iron ~~are~~ welded together was supported by four 475 mm long legs. These were arc welded to the corner s of the square structure. The legs were inclined at 15° from vertical for stability; thereby giving a stand floor base of 525 mm x 525 mm. The total height of the support stand was 460 mm. At the middle of each side of the square structure, a 6 mm thick L-shaped steel extension was welded in a vertical position so that the flange of the conical inlet section of the fluidized bed reactor could lay on these extensions. Four 8 mm x 30 mm ~~hex~~ head bolts were used to fix the inlet section to the support stand.

The vertical section of the air line was connected to a conical (funnel shaped) inlet section made of 3.2 mm thick stainless steel material. The height of the conical section was 120 mm. ~~Itssides~~ were inclined at 45° from vertical. The bottom and top diameters of the conical section were 63 ~~mm~~ and 255 mm, respectively. A flange (collar) made of 8 mm thick stainless steel ~~waswelded~~ to the upper portion of the funnel. The inner and outer diameters of the flange were ~~255mm~~ and 355 mm, respectively. A thick rubber gasket of 3 mm thickness was used between ~~theflanges~~ of the conical inlet section and the distributor plate to provide good sealing.

The distributor plate was made of 8 mm thick circular steel plate of 355 mm diameter. A circular area of 220 mm diameter was perforated. The total open area of the holes was 1.63% of the bed cross-sectional area. A total of 267 holes of 2 mm diameter each were drilled in the circular plate in the form of rings starting from the center with a pitch of 11.1 mm. To prevent falling of the sand through the holes of the distributor plate, a circular screen of 100 mesh size was point welded to the top of the distributor plate. Five plates having exactly the same open area and same number of vertical holes were manufactured (10° concave, 5° concave, flat, 5°convex and 10° ~~convex~~)and used to test the effect of distributor plate configuration on the pressure drop in the fluidized bed (Figure 2).



Hole diameter = 2 mm

Number of holes = 267

Perforated area = 1.63%

$\Theta = 0^\circ, 5^\circ, 10^\circ$



(a) Convex



(b) Flat



(c) Concave

Figure 2. Type of distributor plates



The main body of the fluidized bed (fluidizing column) was made of a plexiglass cylinder having 255 mm inside diameter and 5 mm thickness. It was constructed in three pieces having lengths of 127.5, 255.0, 382.5 mm (0.5, ~~1.0~~, 1.5 D), respectively. This provided a maximum height of 765 mm. Two flanges made of 8 mm thick circular plates were glued to the top and bottom of each cylinder. The height of the fluidizing column was varied by fitting different sections of varying lengths. The sections were bolted to each other and rubber type O-rings of 3 mm thickness were used between them to provide good sealing. A 55 mm diameter port was provided near the bottom of the bed to remove the bed material when required.

To decrease the rate of elutriation from the top of the fluidized bed, an enlarged section was used at the upper part of the bed. This part was made from 3.2 mm thick, hot rolled steel. The sides were inclined at 30° from vertical. The bottom and top diameters were 255 mm and 350 mm, respectively. The total height of this enlarged section, including the inclined part, was 395 mm. The top of this enlarged section was covered with 6 mm thick hot rolled steel, which was connected to the outlet duct.

The outlet duct was made of 1.6 mm thick stainless steel material. The vertical section of the duct was 100 mm in length whereas the horizontal section of the duct was 400 mm in length. The vertical section of the duct had a cross-section of 85 mm x 85 mm at the bed exit whereas the horizontal section has a cross section of 80 mm x 40 mm at the cyclone inlet.

## 2.2. Air Supply

The air supply system consisted of: (a) a blower equipped with a filter, (b) a pressure gauge, (c) a main valve, (d) a by-pass valve, (e) an air line and (f) a flow meter. A blower (Model Engenair R43 1 OA-2-220 volts and 13.4 amps Benton Harbour, MI, USA) having a maximum flow rate of 81.2 L/s was used. The blower was powered by a 4.8 hp, 3 phase electric motor (Blador Industrial motor, 5711, Fort Smith, Arizona, USA) and ran at a speed of 2850 rpm. The maximum pressure that can be obtained from the blower was 212 cm H<sub>2</sub>O (2.08 kPa). A filter having a pore size of 25 µm and a maximum flow of 7.08 m<sup>3</sup>/min was used at the blower inlet to filter the incoming air in order to supply dust and water free air to the fluidized bed reactor. The air line, through which the air was supplied to the fluidized bed, was composed of horizontal and

vertical steel pipe sections. The horizontal section on which the flow meter and main valve were mounted was connected to a 600 mm long horizontal steel pipe having an inner diameter of 63 mm. This was connected to a 100 mm long vertical pipe by a 90° elbow having the same inner diameter. The bypass valve was located on the vertical pipe. A pressure gauge (USG) having a pressure range of 0-690 kPa with a scale of 13.8 kPa increments was used at the exit of the blower to check the pressure level in the air supply line in order to maintain atmospheric pressure in the bed. The main valve was used to control the airflow rate while the by-pass valve was used to by-pass the excess air to avoid over heating of the motor.

The flow rate of the fluidizing air was measured using Flow Cell Bypass Flowmeter (a FLT type Cole Parmer Catalog No. N03251-60, Chicago, IL). This flowmeter is accurate to 2.5 percent of full scale and can be used up to maximum temperature and pressure of 60 °C and 1035kPa, respectively. Three flow meters (with different ranges 2.4-11.8, 5.6-25.5 and 11.8-52.1 L/s) were used depending on the required air flow rate. Each flowmeter was installed in a horizontal pipe having the same flowmeter size rating. The length of the pipe section downstream the flowmeter was kept greater than three times the diameter of the pipe whereas that upstream the flowmeter (after the valve) was greater than eight times the diameter of the pipe.

### 2.3. Cyclone

A cyclone connected to the outlet duct was used to capture the fine solid particles escaping from the top of the bed. The cyclone was made from a 2 mm thick stainless steel metal sheet. It consisted of a conical and a cylindrical section. The cylindrical section had a 150 mm diameter and a 300 mm height. The conical section had a 300 mm height and its sides were inclined at 100° from the vertical. A gas outlet pipe of 75 mm diameter was extended 90 mm axially into the cyclone. At the bottom of the cyclone, the fine dust particles were collected in a cylindrical plexi-glass dust collector of a 60 mm diameter and a 200 mm height.

### 2.4. Pressure Drop Measurement System.

The pressure drop was measured at different heights of the fluidized bed using vertically mounted U-tube manometers. The first measurement point was located in the bed (50 mm above the distributor plate) was used to measure the pressure drop across the distributor plate. The

second and third measurement points were located in the freeboard, 600 and 720 mm above the distributor plate, respectively. The fourth measurement point was located on the outlet duct, connecting the bed exit to the cyclone. All of these pressure measurements were done with respect to a reference point located at the conical inlet section (50 mm below the distributor plate). All five U-tubes were mounted on a vertical plate. Coloured water was used as the manometer liquid. Each measurement point was connected to a different U-tube using flexible, tygon tubing of 10 mm diameter. The other end of the U-tube was connected to the reference point through a manifold.

### 3. EXPERIMENTAL PROCEDURE

#### 3.1. Experimental Design

In this study, the effects of 5 parameters on the pressure drop were investigated. The experimental parameters are shown in Table 1. These were: (a) pressure drop location, with 4 levels, (b) type of distributor plate, with 5 levels, (c) sand mean particle size, with two levels, (d) bed height, with 4 levels and (e) fluidizing velocity, with 4 levels. Three measurements were taken during each experimental run.

#### 3.2. Determination of Particle Size

Two types of sand were used in the study: fine and coarse. The most common method used to measure the size of irregular particles larger than 75  $\mu$ m is sieving (Geldart, 1986). Sieving operation was performed for both types of the sand used in the experiments. After sieving the mean size of the particles was determined using the following equation:

$$d_p = \frac{1}{\sum \frac{x_i}{d_{pi}}} \quad (7)$$

Where:

$d$  = Mean size of the particles ( $\mu$ m)

$x_i$  = Weight fraction of powder of size (-)

$d_{pi}$  = Mean sieve size of a powder ( $\mu$ m)

257 Table 1. Experimental parameters

<b>1. Distributor Plate</b>			
Hole diameter (mm)	$d_{or}$	=	2.000
Pitch (mm)	$p$	=	11.200
Percent perforated area (%)	$f_A$	=	1.647
Plate angle (°)	$\theta$	=	5° concave, 10° concave, flat, 5° convex and 10° convex
<b>2. Sand Particle Size</b>		Fine	Coarse
Mean diameter, $d_p$ (μm)		198.0	536.0
Particle density $\rho_p$ (kg/m <sup>3</sup> )		2600.0	2600.0
Minimum fluidization velocity, $U_{mf}$ (cm/sec)		4.2	26.0
<b>3. Bed Height</b>			
Column inner diameter (cm)	$D$	=	25.50
Freeboard height (cm)	$FB$	=	50.00
Disengagement height (cm)	$DE$	=	39.50
Packed bed height (cm)	$H$	=	0.5 D, 1.0 D, 1.5 D, 2.0 D
<b>4. Fluidizing velocity (FV)</b>			
Fluidizing gas	Air		
Room temperature (°C)	20-22		
Fluidization velocity (cm/s)	$U_o = 1.25 U_{mf}, 1.50 U_{mf}, 1.75 U_{mf}, 2.00 U_{mf}$		
<b>5. Pressure Drop Locations (XX)</b>			
Reference point under distributor plate	5 cm		
Measurement location above distributor plate	5 cm, 60 cm, 72 cm, 132 cm		

258

259

The particle size distributions of the fine and coarse sands are given in Table 2 and represented in Figure 3.

### 3.3. Determination of Pressure Drop across the Distributor Plate

The pressure drop across the distributor plate (PD) was taken to be 10% of the pressure drop across the bed (PB). The pressure drop across the bed (PB) was determined from Equation 2. Reynolds number for the total flow approaching the plate was calculated and the corresponding value for the orifice coefficient ( $C_d$ ) was selected according to the procedure described by Kunii and Levenspiel (1977). The velocity of fluid through the orifices ( $U_o$ ) was determined as follows:

$$U_o = C_d \frac{0.5}{\rho_g} \quad (8)$$

Where:

- $U_o$ = Gas velocity through the orifices (m/s)
- $P_D$ = Pressure drop across the distributor (KPa)
- $C_d$ = Discharge coefficient (-)

The fraction of open area was found from the ratio  $U_o/U_s$ . Deciding on the orifice diameter( $d_o$ ), the corresponding number of orifices per unit area of distributor plate ( $N_{or}$ ) was determined as follows.

$$N_{or} = \frac{4U_s}{\pi(d_{or})^2 U_o} \quad (9)$$

Where:

- $N_{or}$  = Number of orifices per unit area ( $m^2$ )
- $d_o$  = Diameter of the orifice (m)
- $U_s$  = Superficial gas velocity (m/s)

### 3.4. Determination of the minimum fluidization velocity

The minimum fluidizing velocity was calculated using the following equation (Ergudenler et al., 1997):

286 Table 2. Sand particle size.

Sieve aperture ( $\mu\text{m}$ )		$d_{pi}$ ( $\mu\text{m}$ )	Weight fraction (%)	
Minimum	Maximum		Fine	Coarse
850	1410	1130	0.00	0.77
595	850	723	1.28	34.50
425	595	510	19.95	57.40
297	425	631	23.36	5.85
212	297	254	22.57	0.82
0	212	106	32.84	0.66

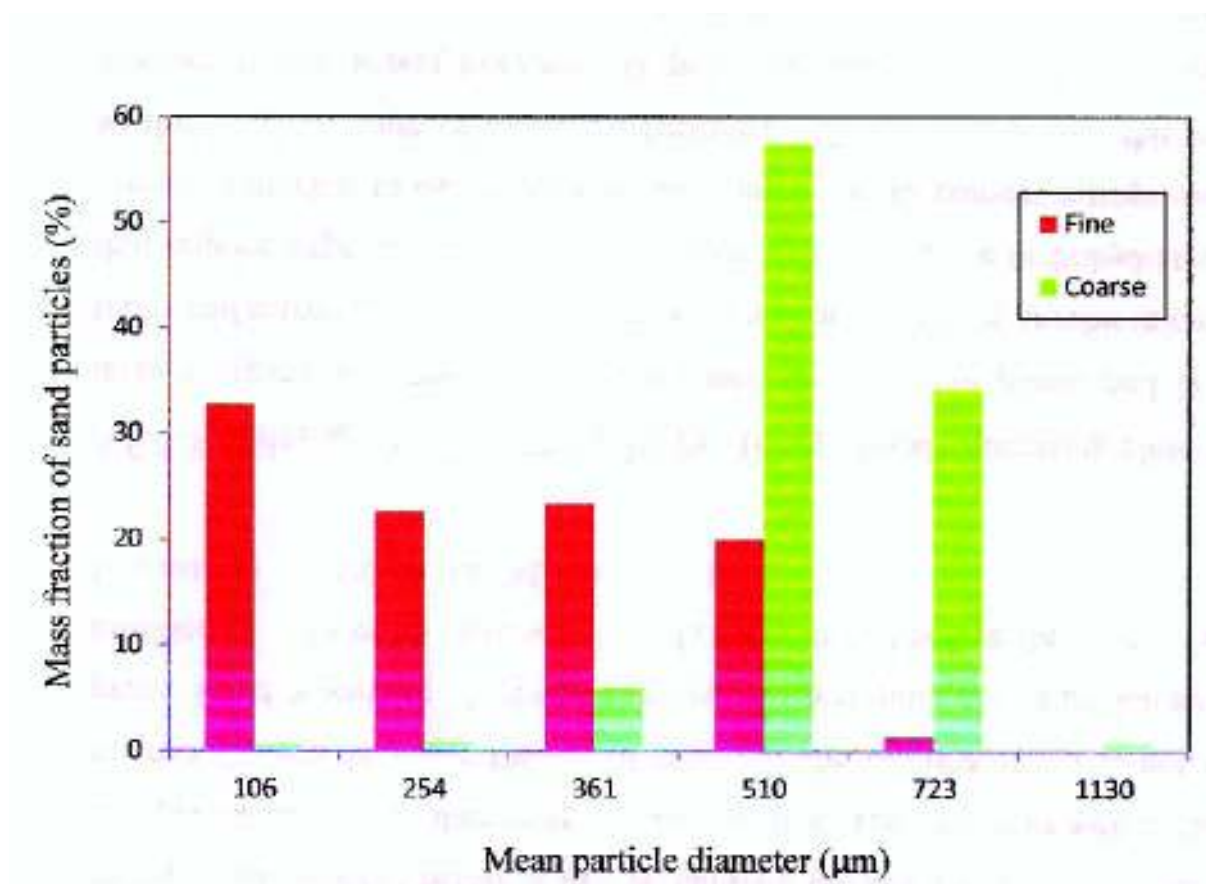
287  $d_p$  = Mean particle size ( $\mu\text{m}$ )

288  $d_{pi}$  = Mean sieve size ( $\mu\text{m}$ )

289  $d_p$  for fine sand = 198  $\mu\text{m}$

290  $d_p$  for coarse sand = 536  $\mu\text{m}$

291



292

293 Figure 3. Sand particle distribution.

$$U_{mf} = \frac{\mu_g}{\rho_p d_p} [C_1^2 + C_2 Ar]^{0.5} - C_1 \quad (10)$$

Where:

$\mu_g$  = Viscosity of the fluidizing gas (g/cm s)

$\rho_g$  = Density of fluidizing gas (g/m<sup>3</sup>)

$\rho_p$  = Density of fluidizing gas (g/m<sup>3</sup>)

$C_1$  = 27.2

$C_2$  = 0.04086

Archimedes number ( $A_r$ ) can be calculated as follows (Gilbilaro, 2001)

$$A_r = \frac{\rho_g d_p^3 (\rho_p - \rho_g) g}{\mu_g^2} \quad (11)$$

### 3.5. Experimental Protocol

The Selected distributor plate was fixed in place and the fluidizing column was assembled. One type of sand (fine sand) was then added to the reactor up to the required bed height. The blower was turned on and the flow rate was adjusted until the required fluidizing velocity was obtained. The pressure differences measured at various points above the distributor plate was recorded. This was then repeated 3 times with a ten minute time interval between measurements. The air flow rate was then changed and the procedure was repeat until three measurements were taken for each of the flow rates.

More sand was then added to the desired bed height and the same procedure was followed until three measurements were obtained for all bed height-flowrate combinations. The sand was changed (course sand) and the above experiments were repeated as with the other type(fine sand)of sand. Finally, the distributor plate was changed and all the above experiments were repeated with all distributor plates.

## 4. RESULTS AND DISCUSSION

The effect of the shape and angle of distributor plate on the pressure drop in a bubblingfluidized bed reactor was investigated at various levels of sand particle size, bed height



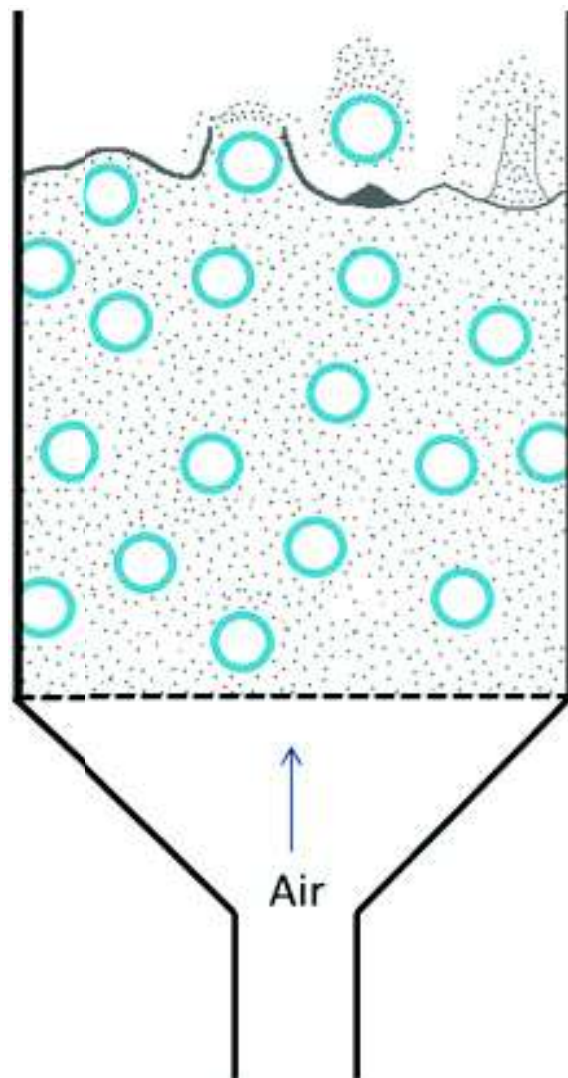
319 and fluidizing velocity. The pressure drop was measured at four locations in the reactor.  
 320 Three pressure drop measurements were taken for each treatment combination.

321 The analysis of the high speed films indicated that vertical transport and mixing of particles  
 322 were achieved by bubble motion as each bubble carried a wake of particles that was ultimately  
 323 deposited on the bed surface (Figure 4). It caused a drift of particles to be drawn up as a spout  
 324 below it as it left the bed of sand. Muller et al. (2007) used particle image velocimetry to capture  
 325 the radial mixing that occurs during bubble burst as shown in Figure 5. When the bubble rises to  
 326 the surface, the bubble roof breaks down and the bubble erupts. The bubble wake is ejected from  
 327 the surface and then falls. The surface appears settled till another bubble erupts.

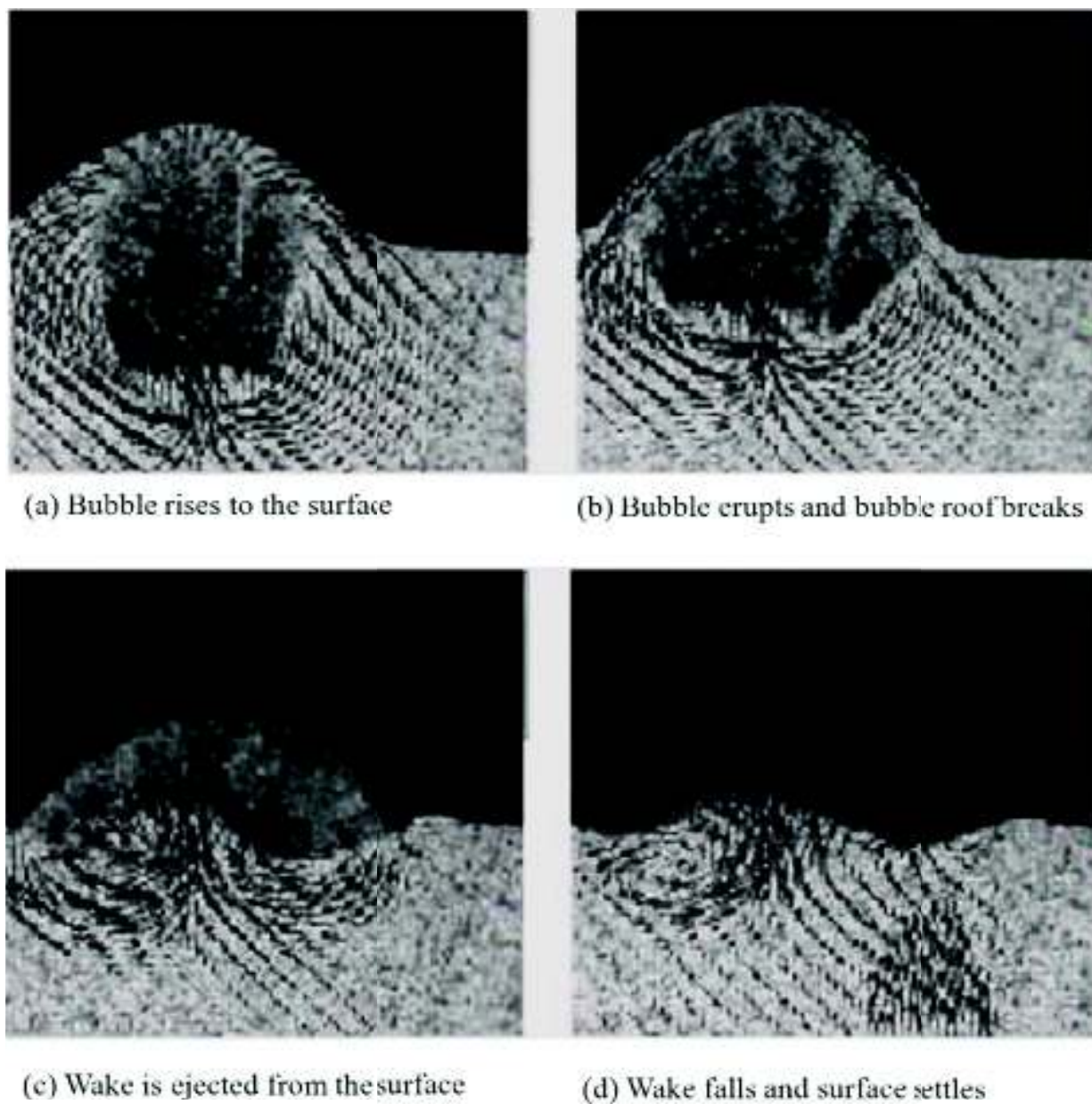
328 The shape (concave, convex or flat) and the angle of the distributor affected the vertical and  
 329 localized mixing as well as the upward/downward movement of sand particles (Figure 6). With  
 330 the convex distributor plate, there was an observed upward movement close to the wall of the  
 331 fluidizing column. These resulted in a completed bed material turn over in addition to the  
 332 localized mixing caused by the bubbles movement. The surface of the expanded material took a  
 333 concave shape and the degree of curvature was affected by the distributor plate angle. When  
 334 using the concave distributor plate the upward movement was observed at the center which also  
 335 resulted in a complete bed material turn over. The surface of the expanded bed material took a  
 336 concave shape and the degree of curvature was also affected by the distributor plate angle of  
 337 concave. The flat distributor plate achieved good fluidization and a uniform bed material  
 338 expansion. Localized mixing caused by the upward movement of the bubbles was clearly evident  
 339 but no bed material turnover was observed.

340 An analysis of variance was performed on the data as shown in Table 3. The effects of  
 341 five variables (the sand particles size, the bed height, the distributor plate angle, the  
 342 fluidizing velocity and the location of measurement) were highly significant at the 0.001 level. The  
 343 analysis of variance also showed that the interactions between the various variables were  
 344 highly significant at the 0.001 level.

345 In order to test the differences among the levels of each of the variables, Duncan's  
 346 **MultipleRange** Test was carried out on the data. The results are shown in Table 4. The 0° convex  
 347 and 10°

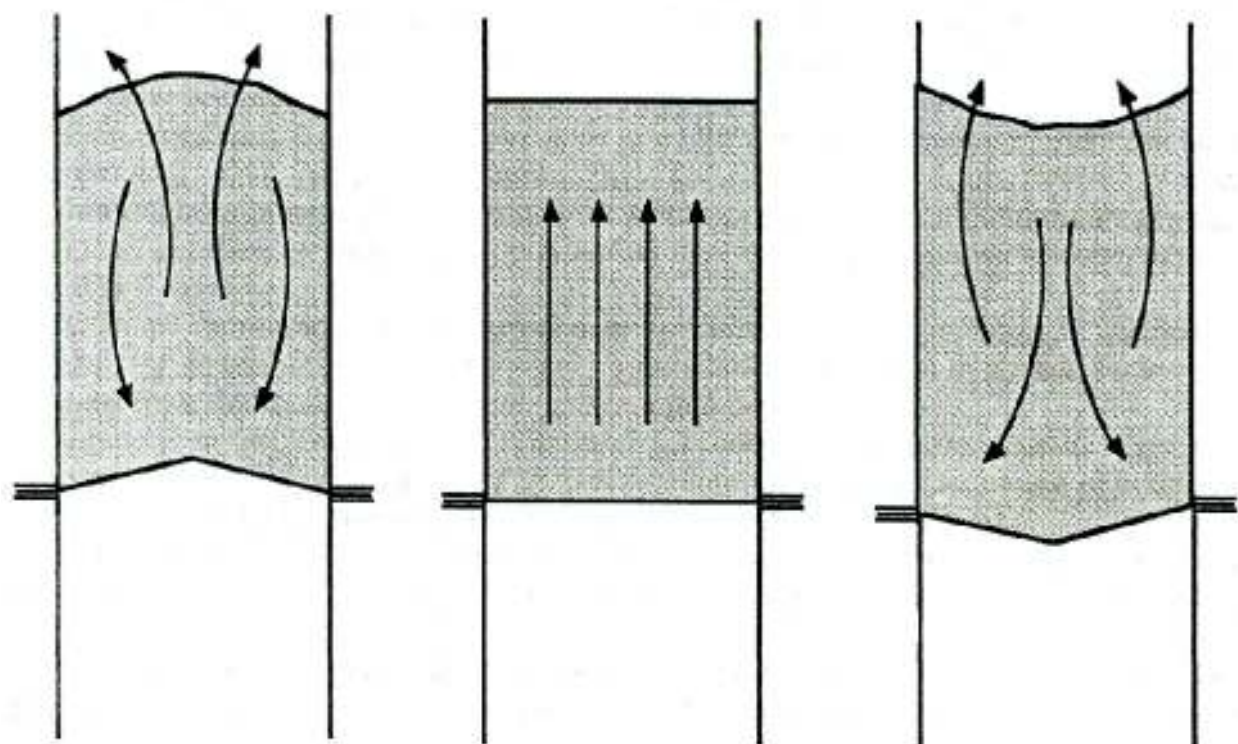


348  
 349 Figure 4. Bubble ejection stages.



350

351 Figure 5. Bubble wake ejection (Muller et al., 2007).



(a) Convex

(b) Flat

(c) Concave

Figure 6. Effect of distributor plate on the mixing pattern in a bubbling fluidized bed.

356 Table 3. Analysis of variance

Source	DF	SS	MS	F	PR>F
TOTAL	359	502617.69			
MODEL	319	502427.47	1575.01	5299.15	0.001
DF	4	8036.32	2009.08	6759.60	0.001
PS	1	28754.70	28754.70	96745.93	0.001
BH	3	177328.37	591109.46	99999.99	0.001
FV	1	1224.92	1224.92	4124.27	0.001
XX	3	222981.51	74327.17	99999.00	0.001
DP*PS	4	3167.70	791.92	2664.45	0.001
DP*BH	12	178.79	14.90	50.13	0.001
DP*FV	4	111.25	27.91	93.57	0.001
DP*XX	12	109.80	9.15	30.79	0.001
PS*FV	1	616.00	616.00	2072.55	0.001
PS*XX	3	2.83	0.94	3.18	0.237
BH*FV	3	13.66	4.55	15.33	0.001
BH*XX	9	58312.73	6479.19	21799.41	0.001
FV*XX	3	5.00	1.66	5.61	0.001
DP*PS*BH	12	307.29	25.61	86.16	0.001
DP*PS*FV	4	12.97	3.24	10.91	0.001
DP*PS*XX	12	137.93	11.49	38.67	0.001
DP*BH*FV	12	100.31	8.36	28.12	0.001
DP*BH*XX	36	154.75	4.30	14.46	0.001
DP*FV*XX	3	2.02	0.67	2.27	0.001
DP*BH*FV	3	38.44	12.81	43.11	0.001
PS*BH*XX	9	30.98	3.44	11.58	0.001
BH*FV*XX	9	20.85	2.31	7.79	0.001
DP*PS*BH*FV	12	52.98	4.41	14.85	0.001
DP*BH*FV*XX	48	47.66	0.99	3.34	0.001
DP*PS*BH*XX	36	59.33	1.64	5.54	0.001
PS*BH*FV*XX	9	25.25	2.81	9.44	0.001
DP*PS*BH*FV*XX	48	77.81	1.62	5.45	0.001
ERROR	640	190.22	0.29		

357  $R^2 = 0.99$ 358  $CV = 1.34\%$ 359  $S_p$  = Particle size

360 DP = Distributor plate

361 BH = Bed Height

362 FV = Fluidization velocity

363 XX = Location of measurement

364

Table 4. Mean values of pressure drop as affected by the angle and shape of distributor plate, particle size, bed height, fluidization velocity and location of measurements.

Parameter	Number of observations	Mean pressure drop	Grouping
<b>Distributor plate angle</b>			
10° convex	192	44.53	A
5° convex	192	40.47	B
Flat	192	39.53	B
5° concave	192	38.23	B
10° concave	192	36.47	A
<b>Particle size (µm)</b>			
198	480	35.06	A
536	480	46.00	B
<b>Bed height (cm)</b>			
0.5D	240	22.45	A
1.0D	240	34.30	B
1.5D	240	46.44	C
2.0D	240	58.92	D
<b>Fluidization velocity</b>			
1.50 $U_{mf}$	480	39.39	A
1.75 $U_{mf}$	480	41.66	B
<b>Location</b>			
P1	240	14.13	A
P2	240	49.32	B
P3	240	49.31	B
P4	240	49.34	B

Means with different letter are significantly different at 0.05 percent level

D = Inner diameter of the fluidizing column (cm)

$U_{mf}$  = Minimum fluidizing velocity

velocity of  $1.75 U_{mf}$ . The first bed location above the plate ( $P_1$ ) was significantly different from the other 3 locations ( $P_2$ ,  $P_3$  and  $P_4$ ) while these three locations were not significantly different from each other at the 0.05 level. The highest pressure drop was observed at the fourth location ( $P_4$ ).

#### 4.1. Effect of Plate Shape

The results showed that there were no significant differences between pressure from measurements across the five distributor plates taken when the bed was empty (i.e. no sand in the bed). However, with the fluidized bed a decrease in the angle of concave and an increase in the angle of convex decreased the pressure drop as shown in Figure 7. It appears that the shape (angle) of distributor plate affected the average bed height (Figure 8) thereby, affecting the pressure drop.

Svensson *et al.* (1996) investigated the influence of fair distributor design on the bubble rise velocity and frequency and pressure drop of circulating fluidized bed. They reported that pressure drop across the distributor was the only significant factor affecting the fluidizing regime. Increasing the pressure drop across the distributor lead to increases in bubble size and rise time resulting in reduced residence time.

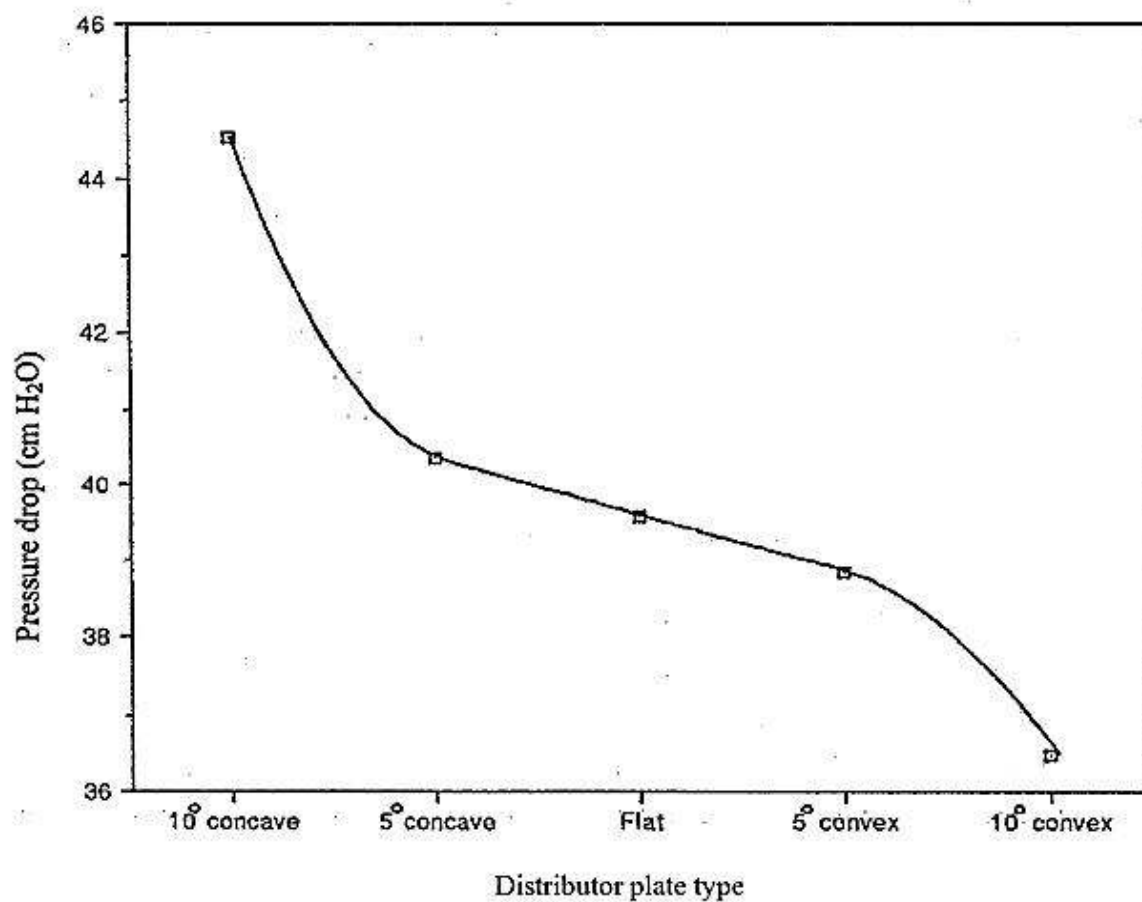
Sobrinho *et al.* (2009) conducted a study for measuring the distributor pressure drops in two types of distributors including perforated plate and bubble cap distributor. The results indicated that the pressure drop in the perforated plate distributor was due to the presence of mesh which was sandwiched between the two plates. Whereas, the pressure drop across bubble cap distributor is mainly due to the resistance to the flow in the entrance orifice.

#### 4.2. Effect of Sand Particle Size

Greater values of pressure drop were obtained with the larger (536 mm) sand particle size (coarse sand) as compared to those obtained with smaller (198 mm) sand particle size (fine sand). On the average, pressure drops of 46.00 and 36.06 were obtained with the coarse and fine sand, respectively. This is due to the difference in minimum fluidization velocity of the fine sand (4.2 cm/s) from that of the coarse sand (26.0 cm/s). The pressure drop across a



399 **bubblingfluidizedbed** has a direct relationship with the minimum fluidization velocity of the  
 400 particles in the bed.

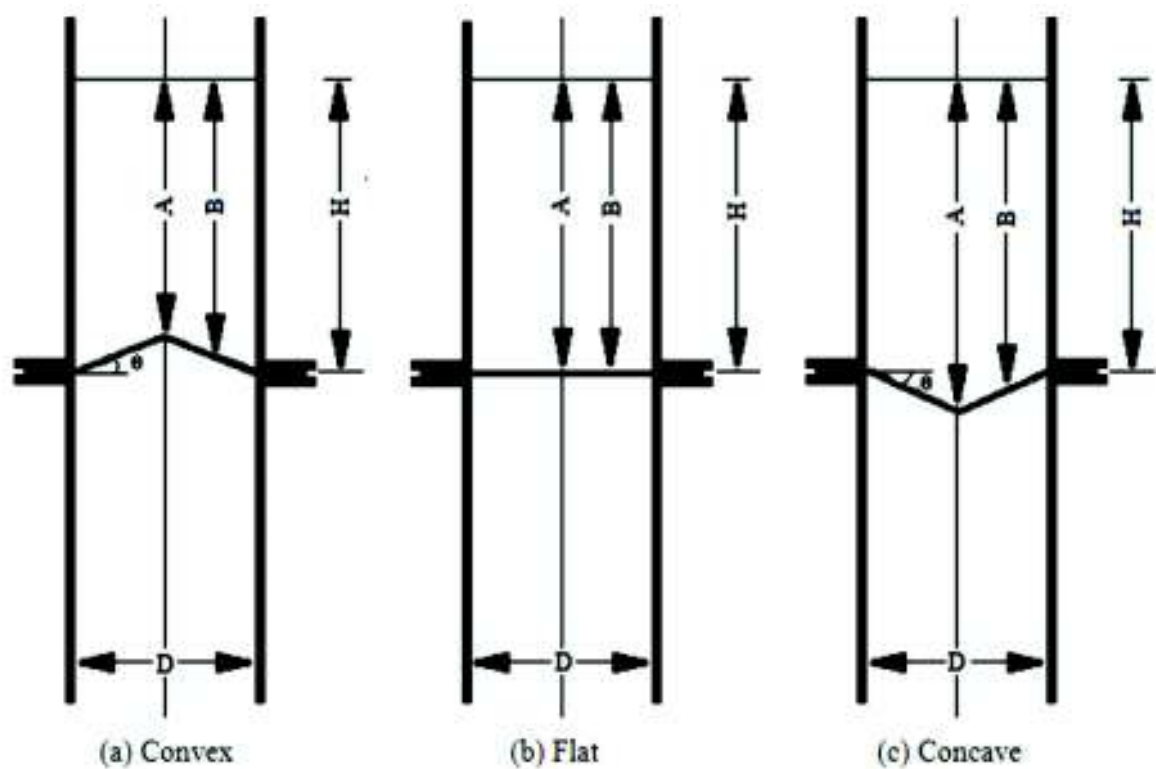


401

402 Figure 7. Effect of distributor plate on pressure drop.

403





$\theta$	A	B
5	$H-1.12 \text{ cm}$	$H-0.56 \text{ cm}$
10	$H-2.24 \text{ cm}$	$H-1.12 \text{ cm}$

$$A=B=H$$

$\theta$	A	B
5	$H+1.12 \text{ cm}$	$H+0.56 \text{ cm}$
10	$H+2.24 \text{ cm}$	$H+1.12 \text{ cm}$

Figure 8. Effect of distributor plate on the vertical transport of the tracer particles.

in the bed. Particles with higher minimum fluidization velocities have greater pressure drop across the bed than particles having lower minimum fluidization velocities.

Guathier et al. (1999) reported that particle size distributions have a strong influence on various fluidization characteristics including fluidization velocity and pressure drop. The study was carried out using four powders (narrow cut, binary mixture, Gaussian and wide cut) with different particle sizes ranging from 282.5  $\mu\text{m}$  to 1800  $\mu\text{m}$ . The authors found that a wide range of particle size has very different fluidization characteristics than powder with a narrow range of particle size. The results from the study indicated that increasing the particle diameter (size) increased the minimum fluidization velocity ( $U_{mf}$ ) constantly and thereby increasing the total pressure drop across the bed.

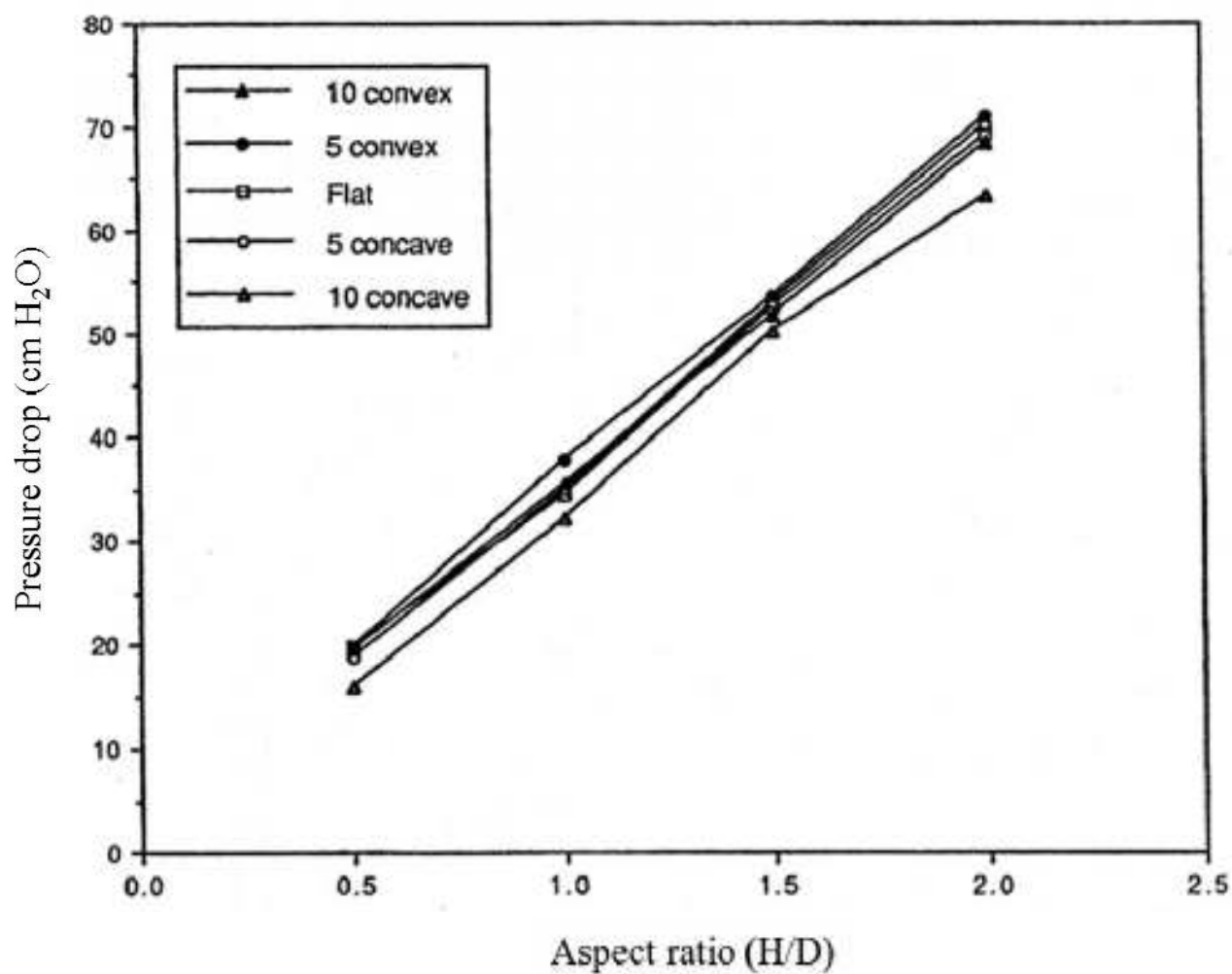
Lin et al. (2002) studied the effect of particle size on fluidization using four different types of powder including: a narrow powder, a binary mixture, a flat and Gaussian distribution powder. The results indicated that particles with higher fluidization velocities tend to segregate and increased the pressure drop across the bed. The results also showed that binary and flat powder had higher minimum fluidization velocities ( $U_{mf}$ ) and segregated and increased the pressure drop across the bed, but narrow and Gaussian distribution powder had lower minimum fluidization velocities ( $U_{mf}$ ) and were readily available for complete mixing.

### 4.3. Effect of Bed Height

An increase in the bed height increased the aspect ratio and as a result increased the pressure drop considerably. The relationship between the bed height and the aspect ratio was linear as shown in Figure 9. The value of the pressure drop varied from a low of 15.45 mm  $\text{H}_2\text{O}$  to a high of 70.92 mm  $\text{H}_2\text{O}$ , depending on the bed height and the distributor plate used. The pressure drop is a function of the weight of particles in the bed. Since the bed diameter is constant, an increase in bed height results in an increase in pressure drop. Similar findings were reported by Trivedi and Rice (1966) and Qureshi and Creasy (1979).

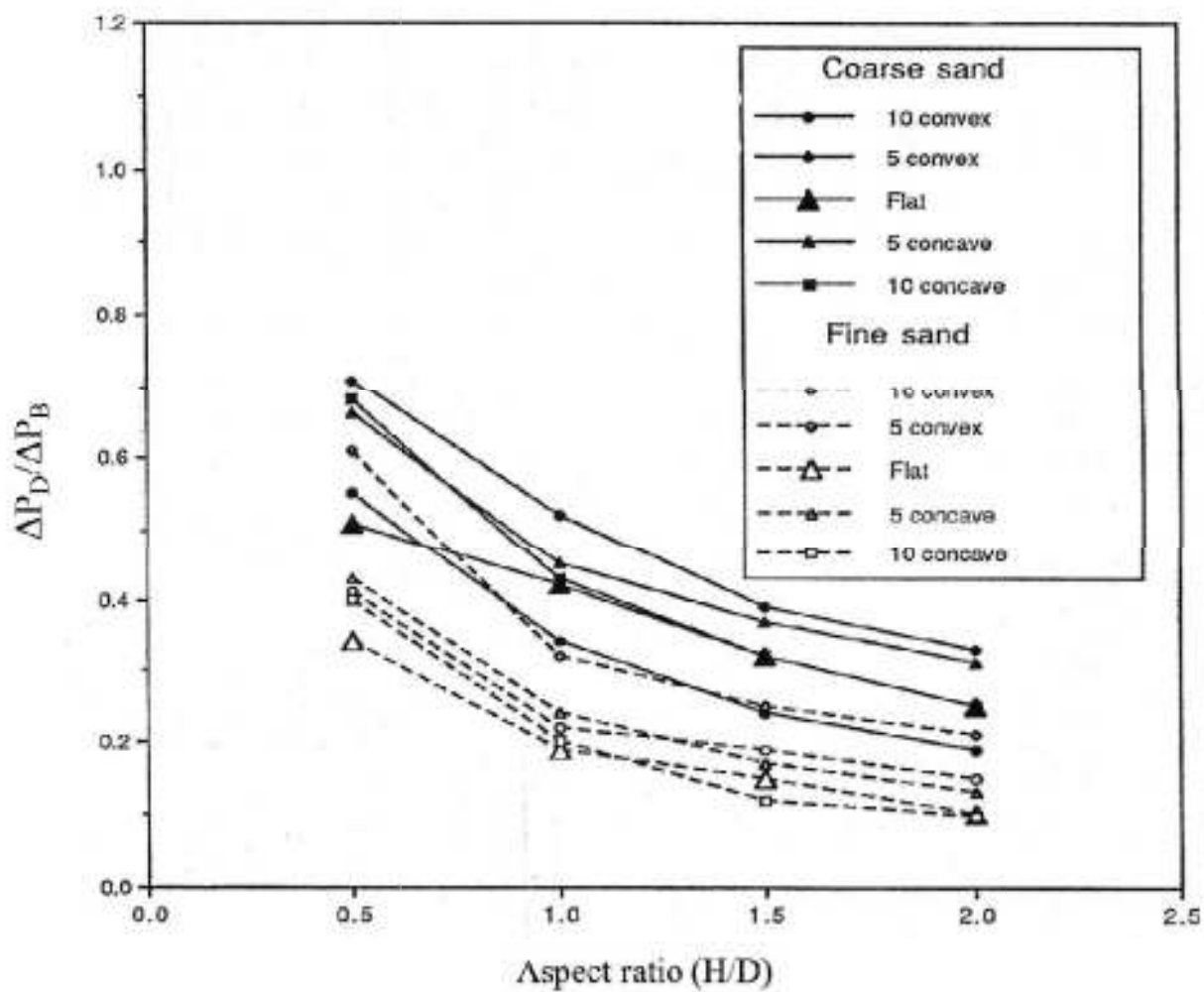
The ratio of the pressure drop across the distributor plate to that across the bed ( $P_D/P_B$ ) decreased with the increase in bed height. Figure 10 shows the variation of the ratio of

434 the experimental pressure drop to the theoretical pressure drop ( $P_E/P_T$ ) with the aspect ratio at  
 435  $U/U_{mf}$



436

437 Figure 9. Effect of aspect ratio on the pressure.



438

439 Figure 10. Effect of aspect ratio on  $\Delta P_D/\Delta P_B$ .

440

=1.75 for the two sizes of sand particles used in the experiments. The pressure drop **ratio decreases** with the increase in bed aspect ratio for all distributor plates. Similar results **were obtained** with other fluidizing velocities. This agrees with the finding of Qureshi and Creasy (1979) and Geldart and Baeyens (1985).

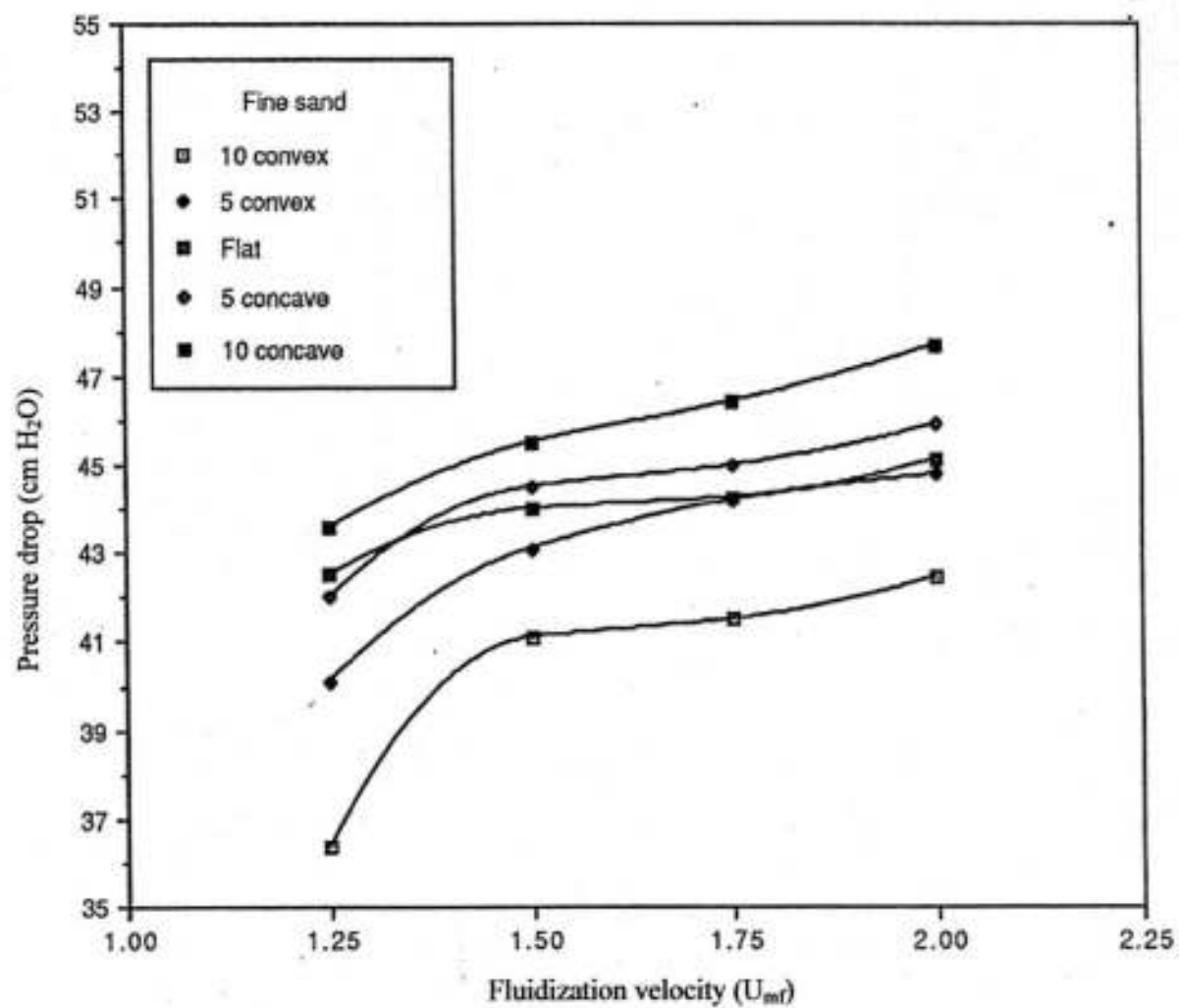
Gelperin *et al.* (1982) studied the variation in **fluidization along** an angled distributor plate and found **the minimum** fluidization velocity to vary from a **minimum value** at the site of the lowest bed height (highest point **of distributor** plate) to a maximum at the site of the **greatest bed** height (lowest point of the distributor plate). **This variation** created a gradient in the effective fluidization velocity and pressure experienced in different regions of the bed.

Taghipour *et al.* (2005) reported that initially the bed height increased with bubble formation and then levelled off at the steady state. As a result, the bed overall pressure drop increased significantly at the beginning of fluidization and then fluctuated for about 3 s. Bi *et al.* (1995) reported that bed oscillations were triggered by the disturbance in the gas flow due to ~~which~~ the bed height increased and settled after the disturbance was cut off. The authors suggested that pressure variations did not result from bed height variations, instead it resulted due to the relaxation of layers of particles after they were displaced from their original positions.

Sathiyamoorthy and Horio (2003) reported that pressure drop across a distributor is conventionally expressed as its ratio to bed pressure drop ( $\Delta P_D/\Delta P_B$ ) and it is in the range of 0.1-0.4 for a uniform operation. The authors suggested that in a deep fluidized bed, the pressure drop is high and gas bypasses as large bubbles or slugs, which affect heat and mass transfer rates. In a shallow the bed, the pressure drop is low as it has a low transport disengaging height and high ~~a~~ solid expansion ratio. The results from the study indicate that the bed pressure ratio ( $\Delta P_D/\Delta P_B$ ) decreases with increases in aspect ratio and it increases with operating velocity.

#### 4.4. Effect of Fluidization Velocity

The mean value of the pressure drop was increased when the fluidization velocity was increased from 1.25 to 1.50  $U_{mf}$  as shown in Figure 11. Further increases in the pressure **drop at** high fluidizing velocity were very small. Generally, the pressure drop should **not increase** with increases in fluidizing velocity and the increase in pressure drop with increased fluidization



469

470 Figure 11. Effect of fluidizing velocity on the pressure drop.

471

velocity observed in this study was more or less within experimental accuracy for [air](#)  
 distributor plates. This suggests that fluidizing velocities higher than  $1.25 U_{mf}$  should be used in  
 order to obtain good fluidization.

Menon and Durian (1997) stated that there are three distinct regimes of behavior observed  
 when velocity ( $U_s$ ) is increased from zero. In the first regime, the values of velocity ( $U_s$ ) are  
 small at constant bed height. At this point, the pressure drops ( $\Delta P$ ) varies linearly with velocity  
 ( $U_s$ ) and depth as per Darcy's law. The bed has similar properties of a static heap of sand with a  
 finite angle of repose at its surface. In the second regime, the velocity ( $U_s$ ) attains minimum  
 fluidization velocity ( $U_{mf}$ ) at which the pressure drops ( $\Delta P$ ) is equal to the weight of the bed and  
 the bed expands homogeneously. At this point, the medium behaves like a fluid and the angle of  
 repose becomes zero and heavier particles sink while the lighter particles float. This is also called  
 as uniformly fluidized state and no intensity fluctuations are seen at this state. The third state is  
 the inhomogeneous state where the velocity ( $U_s$ ) is above the threshold velocity leading the  
 rising up as bubbles with a well-defined interface surrounded by a granular medium having a  
 mushroom-cap shape. In this state, the bed expands with increase in velocity ( $U_s$ ) with no change  
 in pressure ( $\Delta P$ ). In this study, the pressure drop ( $\Delta P$ ) was studied across the fluidized bed at  
 three different particle sizes (49, 96 and 194  $\mu m$ ) and velocity ranging from 0.1 to 10 cm/s. The  
 results indicated that for all particle sizes when the velocity was increased from 0.1 to 10 cm/s  
 the pressure drop increased linearly and the onset of bubbling began at a normalized pressure of  
 1  $\rho gh$ .

Kawaguchi et al. (1998) reported that when pressure drop increases the velocity of gas  
 increases, but the velocity becomes constant at a certain point after which it exhibits overshoot.  
 Inversely, when the gas velocity decreases, the pressure drop remains constant and then starts to  
 decrease when the velocity becomes too low. The minimum fluidization velocity ( $U_{mf}$ ) may be  
 determined by the velocity at which the pressure starts to decrease. In this study the velocity of  
 the gas was gradually increased to 4 m/s and then decreased gradually to 0 m/s and there were  
 high fluctuations in the pressure due to bubbling and slugging and the results were averaged to  
 obtain pressure drop values. The results indicated that the minimum fluidization velocity ( $U_{mf}$ )  
 for the pressure was between 1.7-1.8 m/s. When the gas velocity reached 2.4 m/s the particles  
 began to circulate in the whole region and the bubbles were periodically formed. It was also

noticed that the circulation occurs only at the bottom and the particles at the top were not mixed well and the velocity at the corners was very low compared to those in the other regions. When the velocity was increased to 2.6 m/s there was consistent bubble formations and when the bubble erupts at the surface of the bed, the particles were mixed in the whole region.

#### 4.5. Effect of Location of Pressure Probe

The pressure drop was measured across the distributor plate, at two locations in the freeboard and in the duct leading to the cyclone. There were significant differences among the other three locations in the freeboard and the duct as shown in Figure 12. The two points in the freeboard ( $P_2$  and  $P_3$ ) gave equal pressure drop readings. This is as expected since the flow conditions of the gas-solid stream were not much altered between the two locations. The finding that  $P_4$  is equal to  $P_2$  and  $P_3$  was, however, not expected. Although, the velocity of the fluid increased at the exit due to the smaller area it was forced to pass through, the pressure drop did not decrease. The reason for this is probably that the fluidizing velocities used in these experiments were not great enough to cause a great change in fluid velocity at the contraction that could lead to a detectable decrease in pressure drop.

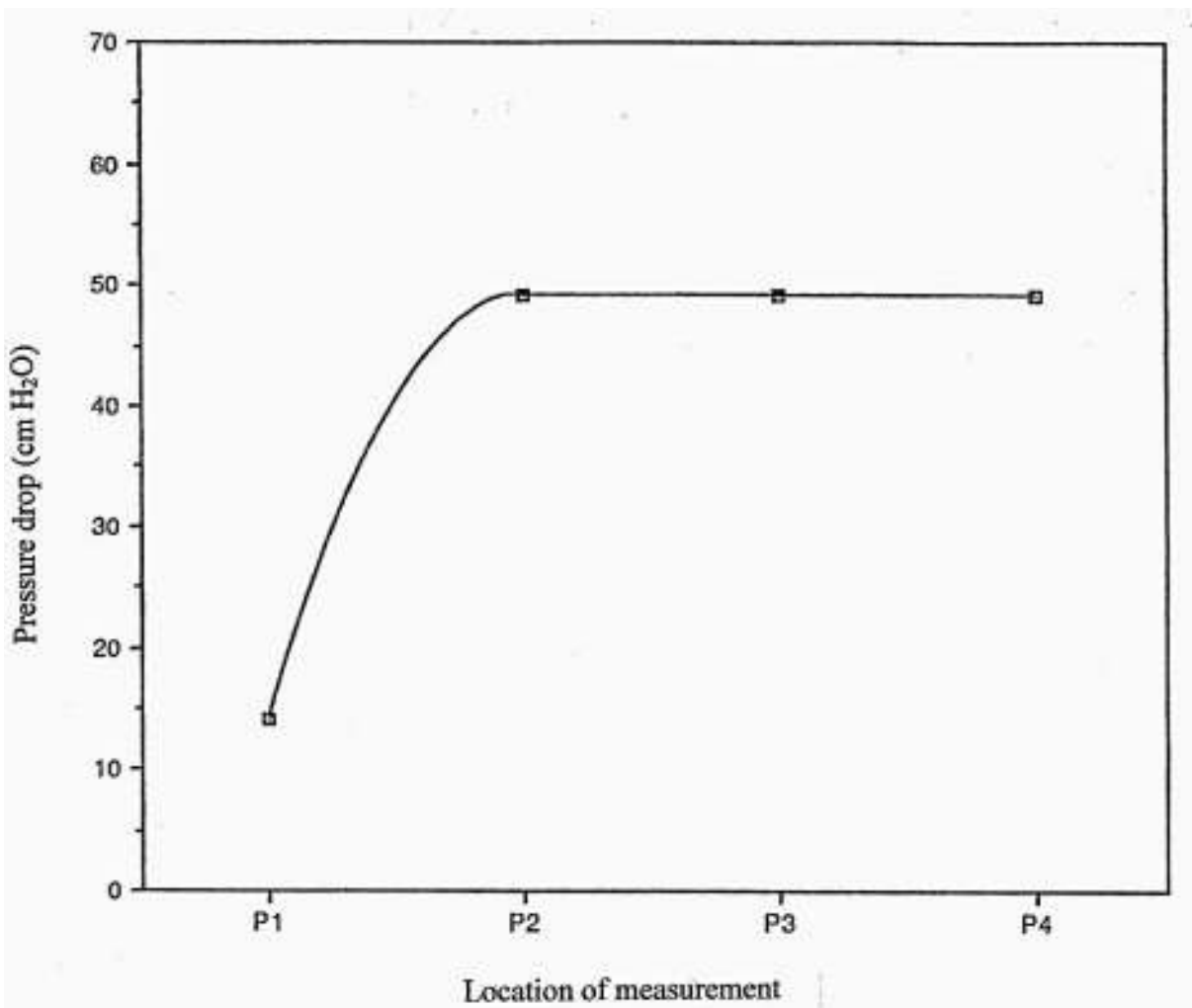
Svoboda et al. (1983) reported that location of pressure probe in the fluidized bed plays an important role. Their results indicated that the maximum amplitude occurred in the middle part of the fluidized bed and the amplitude tend to increase and then decrease with the distance from the distributor were also detected.

Bi and Grace (1995) studied the effect of port spacing and probe location across the fluidized bed. The authors reported that more extraneous pressure waves can be filtered out by reducing the spacing between the probes but the results indicated the velocity was not greatly affected by the port spacing within the test range. The flow of gas across the fluidized bed varied with axial location and different pressure peak points were obtained when the probe was moved to different locations.

## 5. CONCLUSIONS

A pilot scale fluidized bed system was used to study the effect of distributor plate shape and conical angle on the pressure drop. Five distributor plates (flat, concave with  $5^\circ$ , concave with





530

531 Figure 12. Effect of location of measurement on pressure drop.

532

10°, convex with 5° and convex with 10°) were used in the study. The system was tested at two levels of sand particle size (a fine sand of 198  $\mu\text{m}$  and coarse sand of 536  $\mu\text{m}$ ), various bed heights (0.5 D, 1.0 D, 1.5 D and 2.0 D cm) and various fluidization velocities (1.25, 1.50, 1.75 and 2.00  $U_{mf}$ ). The pressure drop was affected by the shape and the conical angle of distributor plate, sand particle size and bed height. Less than theoretical values of the pressure drop were observed with the 10° concave distributor plate at lower fluidizing gas velocities for all bed heights. A decrease in the angle of convex and an increase in the angle of concave resulted in a decreased pressure drop. Greater values of pressure drop were obtained with larger sand particles than those obtained with small sand particles at all fluidizing velocities and bed heights. For all distributor plates, increasing the bed height increased the pressure drop but decreased the ratio of pressure drop across the distributor to the pressure drop across the bed ( $\Delta P_D/\Delta P_B$ ). There was no variation in the pressure drop in the freeboard. Fluidizing gas velocities higher than 1.25  $U_{mf}$  should be used to for a better fluidization, improved mixing and avoiding slugging of the bed.

## REFERENCES

- Basu, P. 2006. Combustion and Gasification in Fluidized Beds. Taylor and Francis Group, LLC, Florence, Kentucky, USA.
- Bi, H. T., J. R. Grace and J. Zhu. 1995. Propagation of pressure waves and forced oscillations in gas solid fluidized beds and their influence on diagnostics of local hydrodynamics. Powder Technology, 82: 239-253.
- Bonniol, F., C. Sierra, R. Occelli and L. Tadrist. 2009. Similarity in dense gas-solid fluidized bed, influence of the distributor and the air-plenum. Powder Technology, 189: 14-24.
- Clift, R. 1986. Hydrodynamics of Bubbling Fluidized Beds in Gas Fluidization Technology (Ed. D. Geldart). John Wiley and Sons, New York, New York, USA.
- Ergudenler, A. and A. E. Ghaly. 1992. Quality of gas produced from wheat straw in a dual distributor fluidized bed gasifier. Biomass and Bioenergy, 3: 419-430.

- 559 Ergudenler, A. and A. E. Ghaly. 1993. Agglomeration of alumina sand in a fluidized bed straw  
560 gasified at elevated temperatures. *Bioresource Technology*, 48: 259-268.
- 561 Ergudenler, A., A. E. Ghaly, F. Hamdullahpur and A. M. Al-Taweel. 1997. Mathematical  
562 modelling of a fluidized bed straw gasifier: Part II- Model sensitivity. *Energy Sources*, 19: 1085-  
563 1098.
- 564 FAO. 2013. Energy for Agriculture. Food and Agriculture Organization of United Nations,  
565 Rome, Italy. Accessed on March 27, 2013.  
566 <http://www.fao.org/docrep/003/X8O54E/x8O54eO5.htm>
- 567 Gauthier, D., S. Zerguerras and G. Flamant. 1999. Influence of the particle size distribution of  
568 powders on the velocities of minimum and complete fluidization. *Chemical Engineering Journal*,  
569 74: 181-196.
- 570 Geldart, D. 1986. Single Particles, Fixed and Quiescent Beds. In: *Gas Fluidization Technology*,  
571 (Ed. D. Geldart), John Wiley & Sons, New York, New York, USA.
- 572 Geldart, D. and J. Baeyens. 1985. The Design of Gas Distributors for Gas Fluidized Beds. *Power*  
573 *Technology* 42: 67-78.
- 574 Gelperin, N.I., V.G. Ainshtein, L.D. Pogorelaya, V.A. Lyamkin and N.I. Terekhow. 1982. Limits  
575 of stable fluidization regimes in vessel with inclined gas distributor grid. *Chemistry and*  
576 *Technology of Fuels and Oils*, 18: 20-24.
- 577 Ghaly, A. E. and K. N. MacDonald. 2012. Mixing patterns and residence time determination in a  
578 bubbling fluidized bed system. *American Journal of Engineering and Applied Science*, 5(2): 170-  
579 183.
- 580 Gibilaro, L.G. 2001. *Fluidization Dynamics*. Elsevier Butter Worth-Heinemann. Waltham,  
581 Massachusetts, U.S.A.
- 582 Goyal, H.B., D. Seal and R.C. Saxena. 2008. Bio-fuels from thermochemical conversion of  
583 renewable resources: A review. *Renewable and Sustainable Energy Reviews*, 12: 504-517.

- 584 Kawaguchi, T., T. Tanaka and Y. Tsuji. 1998. Numerical simulation of two-dimensional  
585 fluidized bed using the discrete element method (comparison between the two and three  
586 dimensional models). Powder Technology, 96: 129-138.
- 587 Khan, A.A., W. deJong, P.J. Jansens and H. Spliethoff. 2009. Biomass combustion in fluidized  
588 bed boilers: Potential problems and remedies. Fuel Processing Technology, 90: 21-50.
- 589 Kunii, D. and O. Levenspiel. 1977. Fluidization Engineering. Kreiger Publishing Company, New  
590 York, USA.
- 591 Lin, C. L., M. Y. Wey and S. D. You. 2002. The effect of particle size distribution on minimum  
592 fluidization velocity at high temperature. Powder Technology, 126: 297-301.
- 593 Mansaray, K. G. and A. E. Ghaly. 1999. Air gasification of rice husk in a dual distributor type  
594 fluidized bed reactor. Energy Sources, 2: 867-882.
- 595 Menon, N. and D. J. Durian. 1997. Particle motions in a gas-fluidized bed of sand. Physical  
596 Review Letters, 79(18): 3407-3410.
- 597 Muller, C.R., J.F. Davidson, J.S. Dennis and A.N. Hayhurst. 2007. A study of the motion and  
598 eruption of a bubble at the surface of a two-dimensional fluidized bed using Particle Image  
599 Velocimetry (PIV). Industrial and Engineering Chemistry Research, 46: 1642-1652.
- 600 Nemtsow, D.A. and A. Zabaniotou. 2008. Mathematical modelling and simulation approaches of  
601 agricultural residues air gasification in a bubbling fluidized bed reactor. Chemical Engineering  
602 Journal, 143: 10-31.
- 603 Pavia, J., C. Pinho and R. Figueiredo. 2004. The Influence of the Distributor Plate on the Bottom  
604 Zone of a Fluidized Bed Approaching the Transition from Bubbling to Turbulent Fluidization.  
605 Chemical Engineering Research and Design 82 (A 1): 25-33.
- 606 Qureshi, A. E. and D. E. Creasy. 1979. Fluidized Bed Gas Distributors. Power Technology, 20:  
607 47-52.

- 608 Rowe, P.N. and A.W. Nienow. 1976. Particles mixing and segregation in gas fluidized beds: a  
609 review. *Powder Technology*, 15: 141-147.
- 610 Sathiyamoorthy, D. and M. Horio. 2003. On the influence of aspect ratio and distributor in gas  
611 fluidized beds. *Chemical Engineering Journal*, 93: 151-161.
- 612 Sobrino, C., N. Ellis, M. de Vega. 2009. Distributor effects near the bottom region of turbulent  
613 fluidized beds. *Powder Technology*, 189: 25-33.
- 614 Sundaresan, S. 2003. Instabilities in fluidized beds. *Annual Review of Fluid Mechanics*, 35: 63-  
615 88.
- 616 Surisetty, V.R., J. Kozinski and A.K. Dalai. 2012. Biomass, availability in Canada, and  
617 gasification: and overview. *Biomass Conversion and Biorefinery*, 2: 73-85.
- 618 Svensson, A., F. Johnsson and B. Leckner. 1996. Fluidization regimes in non-slugging fluidized  
619 beds: The influence of pressure drop across the air distributor. *Powder Technology*, 86: 299-312.
- 620 Svoboda, K., J. Cermak, M. Hartman, J. Drahos and K. Selucky. 1983. Pressure fluctuations in  
621 gas-fluidized beds at elevated temperatures. *Industrial and Engineering Chemical Process*, 22(3):  
622 514-520.
- 623 Taghipour, F., N. Ellis and C. Wong. 2005. Experimental and computational study of a gas-solid  
624 fluidized bed hydrodynamics. *Chemical Engineering Science*, 60: 6857-6867.
- 625 Wood, S.M. and D.B. Layzell. 2003. A Canadian Biomass Inventory: Feedstocks for a Bio-based  
626 Economy. BIOCAP Canada Foundation, Kingston, Ontario, Canada.
- 627 Yoshida, K., H. Kameyama and F. Shimizu. 1980. Mechanism of particle mixing and  
628 segregating in gas fluidized beds. In *Fluidization*, Grace, J.R. and J.M. Matsen, (Eds.). Plenum  
629 Press, New York, New York, USA.